SEGMENTATION AND CLASSIFICATION OF INTRAVASCULAR ULTRASOUND IMAGES FOR PLAQUE DETECTION USING MACHINE LEARNING TECHNIQUES

SYNOPSIS

Submitted for the award of the degree of

DOCTOR OF PHILOSOPHY

IN

ELECTRONICS AND COMMUNICATION ENGINEERING

by

K.V. ARCHANA (Reg. No. 17PHELP002)

Ph.D. Research scholar (Part Time)

Under the guidance of

Dr.R. VANITHAMANI

Professor

Department of Biomedical Instrumentation Engineering

School of Engineering

Avinashilingam Institute for Home Science and Higher Education for Women

Coimbatore

November 2022

SEGMENTATION AND CLASSIFICATION OF INTRAVASCULAR ULTRASOUND IMAGES FOR PLAQUE DETECTION USING MACHINE LEARNING TECHNIQUES

1. INTRODUCTION

Cardiovascular Diseases (CVDs) are among the leading causes of death in most developed nations. According to the experts report of [1], the long-term effects of Covid-19 are likely to influence cardiovascular health, and the global burden of cardiovascular disease will increase exponentially over the next few years. In many cases, CVDs are caused by coronary artery disease: a condition caused by the accumulation of lesions called plaques on the vessels that supply blood to the heart. The pathology of cardiovascular diseases begins with the deposition of lipoprotein cholesterol, thickening of vessel walls, increased levels of vascularization, and the formation of atherosclerotic plaque on the vessel walls [2]. Figure 1(a) represents a longitudinal B-mode ultrasound image of the carotid artery while Figure 1(b) shows a plaque deposited along the carotid artery.

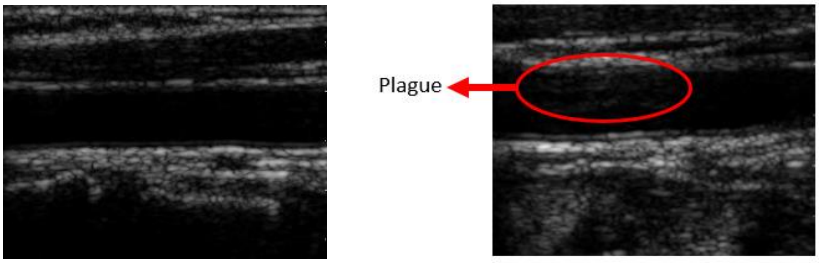

(a) **(b)**

Figure 1 Longitudinal B-mode ultrasound image of carotid artery: (a) Healthy, (b) Plague deposits on the arterial wall

The narrowing of carotid arteries due to plaque formation causes carotid artery stenosis. In some cases, it can progress to complete blockage, resulting in a stroke. The imaging of carotid arteries plays a critical role in diagnosis of carotid artery stenosis and in monitoring plaque progression during treatment.The ultrasound imaging modality has been successfully applied in the past for detecting arterial diseases, and Intravascular Ultrasound (IVUS) imaging has begun to gain attention in the diagnosis of CVD. The IVUS technique uses a catheter equipped with a guided transducer at the tip to obtain cross-sectional views of blood vessels in real time and

provide additional information about plaque deposition. The transducer emits very high frequency sound waves called ultrasound. Ultrasound waves bounce off the various tissue structures of the vessels in the heart and these backscattered waves are converted into images. Coronary arteries are generally divided into three distinct regions. The media constitutes the actual artery wall. Endothelial cells form the intima, which makes direct contact with blood flowing through it. The luminal region is in fact the open channel for blood to flow. In a healthy artery, the intima layer is very thin; however, in a diseased artery, it is thickened by plaque deposition. By segmenting IVUS images, the amount of vessel obstruction and the shape of the plaque deposit can be determined. A number of factors reduce the accuracy of segmentation, and this leads to difficulties in interpreting the disease level.

2. LITERATURE SURVEY

Speckle noise suppression is a vital pre-processing step since the presence of speckle patterns may interfere with the analysis and extraction of features. Numerous researchers have developed various algorithms to suppress speckle noise in the past few years, from simple filters to complicated algorithms. In [1], [2] and [3] some commonly known spatial domain despeckling filters are used. For speckle reduction in ultrasound images, bilateral and Gaussian filters are used in [4] and [5]. Wavelet-based filtering has become increasingly popular among researchers in the last few years. The wavelet types Haar, Daubechies, Symlets, Coiflets, and Biorthogonal are utilized in [6, 7], and [8] for despeckling ultrasound images. In [9, 10], thresholding in the wavelet domain is applied and is proved to be effective.

Recently, a combination of algorithms has been widely used in denoising ultrasound images. An optimization algorithm cascaded with Wiener filter is presented in [11], wavelet and enhanced Kuan filter blended together in [12], and wavelet combined with bilateral filter in [13]. Some despeckling algorithms have demerits that have to be addressed. Different window sizes can affect the output of some despeckling methods [14]. Some filtering techniques require threshold values to be specified in the filtering process that should be estimated empirically; an incorrect selection of threshold may lead to noisy boundaries. Several papers discuss the despeckling algorithms for synthetic aperture radar (SAR) images, satellite images, optical coherence tomography (OCT) images, as well as fetal ultrasound. There are

only a few studies using carotid artery ultrasound. A summary of recent work on despeckling algorithms for carotid artery ultrasound images is listed in Table.1.

Table 1. Comparison of despeckling algorithms for carotid artery ultrasound

Author/Paper	No. of algorithms compared	Comparison Metrics
Rafati, M., et. al. [15]	3	10
Nieniewski, M., et. al. [16]	16	1
Loizou, C.P., et al. [17]	10	9
Yu, Y., [18]	3	3

Even though numerous despeckling algorithms have been proposed in the literature, a systematic comparison of the performance of these filters is still needed. This comparison will facilitate selection of appropriate filters for clinical applications. The first stage of the research compares the performance of ten different despeckling filters for the purpose of removing speckle noise.

A supervised machine learning methods to segment coronary arteries without much human interaction is presented in [15]. Gradient boosting along with quadratic approximation is also implemented. While comparing this system with other learning methods, it has achieved a higher degree of accuracy and Jaccard similarity of 96.8%. Images from real time are used to make the final prediction.

An automated gating algorithm to select end-diastolic frames and bypass saw tooth artifacts in the first stage is presented in [16]. Multi frame CNN is used in the second stage to segment the lumen in the image automatically. At the end of the process, a Gaussian process is applied to the lumen boundary to return to the former state or the less developed state. This proposal reduced the time needed for manual delineation as well as the cost.

In recent studies, it is stated that the composition of plaque is more important than the size of plaque because it is linked to ischemic cardiovascular events. The carotid artery bifurcation is easily accessible and it plays an important role in the development of ischemic stroke. The presence of smaller capillaries and the motion of the heart makes imaging of the wall difficult. Plaque formation in the carotid arteries showed a higher correlation with the composition of atherosclerosis in the carotid bifurcation. The work involved 2666 participants who underwent carotid MRI

examinations. In the assessment, the results obtained were classified according to the Carotid plaque characteristics, the presence of coexisting components, and plaque size [17].

Machine learning-based segmentation has gained prominence in recent years due to its robustness and accuracy. In [18], a U-Net architecture by adding two encoders to detect the shape of IVUS images is implemented. The IVUS dataset consists of 118 images from 101 patients, which has been annotated by radiologists. In the final stage of training the network, 9715 frames are selected. Jaccard Index (JD), Dice Similarity Coefficient (DC), Hausdorff Distance, and Percentage of Area Difference (PAD) are used to evaluate the performance of the proposed model. As far as segmentation of lumen and vessel areas is concerned, the model performed well.

In [19], comparison of Convolutional Neural Network (CNN) and Back Propagation Network (BPN) for segmenting plaque regions are done. CNN architectures are designed with two pooled layers, a fully connected layer, and a SoftMax layer for object recognition and artery wall segmentation. CNN achieved an accuracy rate of 98.12%, which was 1% higher than BPN. A self-learning-based segmentation technique for extracting edges from images is proposed in [20]. In Density-Based Spatial Clustering of Applications with Noise (DBSCAN), the extracted edges are used for pixel segmentation. Particle Swarm Optimisation (PSO) and Gradient Vector Flow (GVF) snake models are used to analyze the results. Compared to manual segmentation, the proposed algorithm is more accurate by 12%.

Boundary-based segmentation methods are prone to error since they are sensitive to gradient variations at the edges. There have been some integrated and dynamic approaches proposed to overcome these drawbacks, which are particular to the datasets that are used for analysis. After segmentation, most articles failed to calculate the thickness of boundary walls, which is useful for further analysis.

For effective plaque detection, it is essential to address the limitations of all the above-mentioned techniques in the current study. The second stage of the research will focus on developing image segmentation algorithms that will improve the classification and accuracy of images.

3. PROBLEM FORMULATION

It is important to detect diseases early to prevent internal organ and tissue damage. Through computer assisted diagnosis (CAD) of intravascular ultrasound images, it is possible to detect heart disease risk at an early stage. Speckle patterns can adversely affect ultrasound images, which can result in poor diagnosis. Although speckles are considered as noise, they contain some valuable information. Despite this, it still limits the contrast resolution of the imaging modality and the effectiveness of diagnosis. Therefore, speckle pattern should be suppressed without adversely affecting image quality.

Ultrasound imaging is a completely manual process, and all parameters are adjusted according to the subjective opinion of the ultrasound operator. It is therefore difficult and requires highly skilled personnel to acquire good quality ultrasound images. The echogenicity depends on the tissue composition, insonation angle, tissue attenuation, and blood flow, regardless of the acquisition protocol. The ultrasound images are affected by local changes in intensity, contrast, and speckle pattern. Thus, it is necessary to suppress speckle patterns before segmentation. Research focuses on analysing carotid ultrasound images for disease diagnosis, starting from image denoising for speckle reduction to segmentation algorithms for extracting the region of interest.

4. OBJECTIVES OF THE RESEARCH

The following are the main objectives of the research

- Identifying the most efficient speckle reduction algorithms for IVUS image noise removal.
- To segment the plaque region using machine learning method (CNN Architecture) and compare the performance of the proposed method with existing algorithms using evaluation metrics such as Jaccard Index (JI), Dice similarity Coefficient (DC), and Hausdorff Distance (HD).
- To classify the IVUS image into diseased and normal one by implementing classifiers such as K-Nearest Neighbour (KNN), Support Vector Machine (SVM), Decision Tree and Bagged Trees.

5. PROPOSED METHODOLOGY

The proposed research aims to detect arthrosclerosis in IVUS images. It is divided into three stages: Pre-processing, Segmentation, and Classification. Figure 2 shows the proposed workflow.

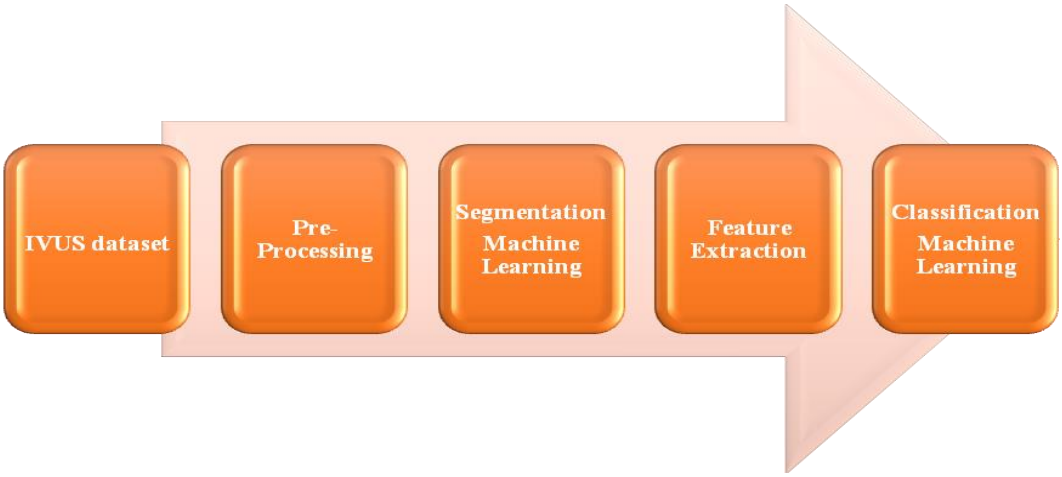

Figure 2 Flow Chart of the Proposed Work

5.1 Pre- Processing

Speckle noise suppression is a crucial pre-processing step, as the presence of speckle patterns may interfere with the process of feature extraction and analysis. Even though many despeckling algorithms have been developed over the years, a systematic comparison of their performance still proves to be very useful. This comparison will facilitate the choice of an appropriate filter for clinical applications. The following filters are implemented to suppress speckle noise in carotid artery ultrasound images in the initial work.

a. **Butterworth Filter**

Butterworth filters are more common in signal processing. They are used for smoothing in the frequency domain in image processing. Speckle noise has a high frequency component, so this filter removes the high frequencies while maintaining the low frequencies [14].

b. **Doubly Degenerative Diffusion (DDD) Filter**

In [21], the DDD algorithm is inspired by nonlinear diffusion models using a slightly modified Fast Explicit Diffusion Scheme (FSDS), as this algorithm is noted to

denoise rapidly. Overall efficiency is increased several times through the use of this technique.

c. **Homomorphic Wavelet Filter**

Homomorphic wavelet filtering involves applying logarithmic transform to the input image followed by discrete wavelet transform. Using wavelet coefficients, the inverse discrete wavelet transformation is used to reconstruct the image, whose exponential is the filtered output [22]. Two levels of filtering are used in this work. Level 1 filtering divides the input image into four sub bands, LL, LH, HL and HH. As most of the speckle noise occurs in the HH band, it is eliminated. During level 2 filtering, the entire process is repeated with the level 1 filtered image as input.

d. **Speckle Reducing Anisotropic Diffusion** (**SRAD) Filter**

The Speckle Reducing Anisotropic Diffusion Filter (SRAD), as it is sometimes known, is an extended version ofanisotropic diffusion filter. SRAD distinguishes edges in images by using the instantaneous coefficient of variation, which provides high values for edges and low values for homogeneous regions. High values decrease the smoothing effect at edges, so edges are preserved to a greater extent and speckle pattern is reduced in homogenous regions [24].

e. **Perona-Malik filter (PM)**

It is a nonlinear anisotropic diffusion method proposed by Perona and Malik in 1990 based on partial differential equations. Over time, variations and improvements have been made to this filtering process. For speckle reduction in ultrasound images, four different versions of PM filters such as Modified PM 1, Modified PM 2 and Adaptive PM proposed in [25] are used.

f. **Total Variation (TV) model**

TV denoising approach is developed to preserve sharp edges while smoothing homogenous regions. The regularization parameter controls the degree of smoothing effect. Numerous The mathematical equation of Total Variance Regularization is given as:

$$T(u) = F(^{b}/_{(A_u)} + \lambda \|\triangle u\|) \quad (1)$$

5.2 Segmentation for Plaque Identification

Deep learning techniques are used for the segmentation of plaques in carotid arteries. In this study, CNN is used as the deep learning model to segment plaques.Deep learning techniques are used for the segmentation of plaques in carotid arteries. This study used CNN as a deep learning model to segment plaques. Four layers were used in the model, namely the input layer, the max-pooling layer, the convolutional layer, and the SoftMax layer. This work uses a 5x5 filter size. The proposed model is illustrated in Figure 3.

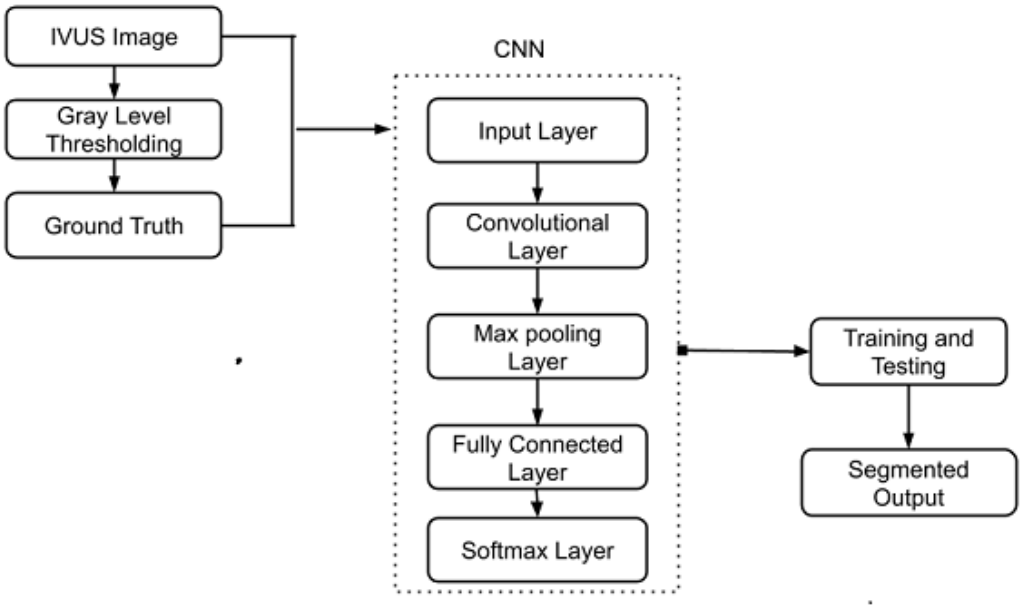

Figure 3 CNN Architecture for Segmentation of Plaque from IVUS images

Following are the steps in the segmentation algorithm:

Step 1: Select a sample image from the IVUS dataset.

Step 2: Extract a ground truth image from the input image by applying a Gray Level threshold to it.

Step 3: Using the dataset of 99 IVUS images, 99 ground truth images are taken.

Step 4: A CNN was trained and tested using 138 images and 60 images, respectively.

Step 5: Testing is done to confirm the performance of the network.

CNN architecture parameters are shown in Table 2.

Table 2 Hyper parameter tuning in CNN Architecture

Parameters	Specifications
Activation Function	**ReLU and SoftMax**
Learning Rate	**0.0001**
Optimiser	Stochastic Gradient Descent with Momentum (**SGDM**)
Mini - Batch Size	**125**
Epochs	**20**
No. of Hidden Neurons	**100**
Fully Connected Layers	**2**

In order to determine the performance of this method, it is compared to existing algorithms such as Fuzzy C Mean Clustering (FCM), Watershed segmentation, Otsu thresholding, Gray level thresholding, K means clustering, and Global region-based segmentation. The performance metrics includes JI, DC and HD are compared with other existing algorithms.

5.3 Classification of IVUS Image

Finally, IVUS images are classified based on statistical measures such as Mean, Standard Deviation, Contrast, Entropy, and Energy. Classifier's performance is evaluated using metrics such as accuracy, sensitivity and specificity. Machine Learning techniques such as KNN, SVM, Decision Trees, and Bagged Trees are used for classification.

6. RESULTS AND DISCUSSION

This section presents the results of the experiments and their analysis using MATLAB programming for plaque detection.

6.1 Pre – Processing Results

The despeckling algorithms are compared based on five image quality metrics: Signal to Noise Ratio (SNR), Peak Signal to Noise Ratio (PSNR), Structural Similarity Index Measure (SSIM), Beta Metric, and Natural Image Quality Evaluator (NIQE). In decibels, PSNR represents the ratio of the maximum value of an image to the power of noise. SSIM compares images on the basis of luminance, contrast, and structure. As such, this metric takes into account the factors of the human visual system. NIQE is a completely blind image quality score that does not require a reference image. In general, a lower NIQE score indicates better perceptual quality. Beta Metric indicates the edge preserving condition in the image. Table 3 displays the metrics that are calculated for all ten filters.

Table 3 Performance Evaluation for Pre-processing

Image 1					
	SNR (dB)	**PSNR (dB)**	**SSIM**	**Beta metric**	**NIQE**
Butterworth	17.0268	28.2049	0.7722	0.0581	5.4423
Homo-wavelet L1	22.4286	32.8915	0.9684	0.7062	4.5548
Homo-wavelet L2	12.2472	19.6408	0.4440	0.2125	6.4660
PM	17.3775	29.7711	0.8165	0.7269	5.2345
Modified PM1	16.9664	28.9839	0.8087	0.4784	5.4375
Modified PM2	19.2578	36.2369	0.9134	0.8865	4.6470
Adaptive PM	21. 2722	39.6659	0.9848	0.6512	4.2170
DDD	22.6201	32.2041	0.9492	0.2414	5.7471
SRAD	20.9932	31.7674	0.8960	0.9678	4.2345
TV	20.0979	33.4916	0.8682	0.4795	5.5907
Image 2					
	SNR	**PSNR**	**SSIM**	**Beta metric**	**NIQE**
Butterworth	16.8482	27.9927	0.7459	0.0703	5.7619
Homo-wavelet L1	22.9840	33.1328	0.9790	0.7363	4.5287
Homo-wavelet L2	11.8141	19.1700	0.3735	0.3053	5.7325
PM	17.0912	29.4471	0.7940	0.7640	5.3577
Modified PM1	16.0410	28.7110	0.7866	0.4987	5.2755
Modified PM2	19.9502	35.5860	0.9017	0.8454	4.7071
Adaptive PM	21.6993	40.0552	0.9832	0.6851	4.8266
DDD	23.8979	32.1440	0.9397	0.2489	5.6164
SRAD	21.0301	32.7303	0.7939	0.9538	4.9373
TV	19.9804	32.3363	0.8466	0.3228	4.7793
Image 3					
	SNR	**PSNR**	**SSIM**	**Beta metric**	**NIQE**

Butterworth	17.9540	28.4858	0.8048	0.0583	5.4984
Homo-wavelet L1	21.9564	32.1224	0.9492	0.7085	4.1570
Homo-wavelet L2	12.4526	19.5022	0.3456	0.3025	5.4028
PM	17. 1324	28.2473	0.7041	0.7242	6.4336
Modified PM1	16.0410	29.8052	0.8561	0.4673	5.2894
Modified PM2	19.6004	35.7642	0.9056	0.8341	5.0543
Adaptive PM	20.2577	39.1341	0.9723	0.6429	4.4003
DDD	23.4903	32.5726	0.9557	0.2184	5.3332
SRAD	20.8342	31.2741	0.8242	0.9619	5.4302
TV	20.9804	32.4317	0.8904	0.3109	5.2967

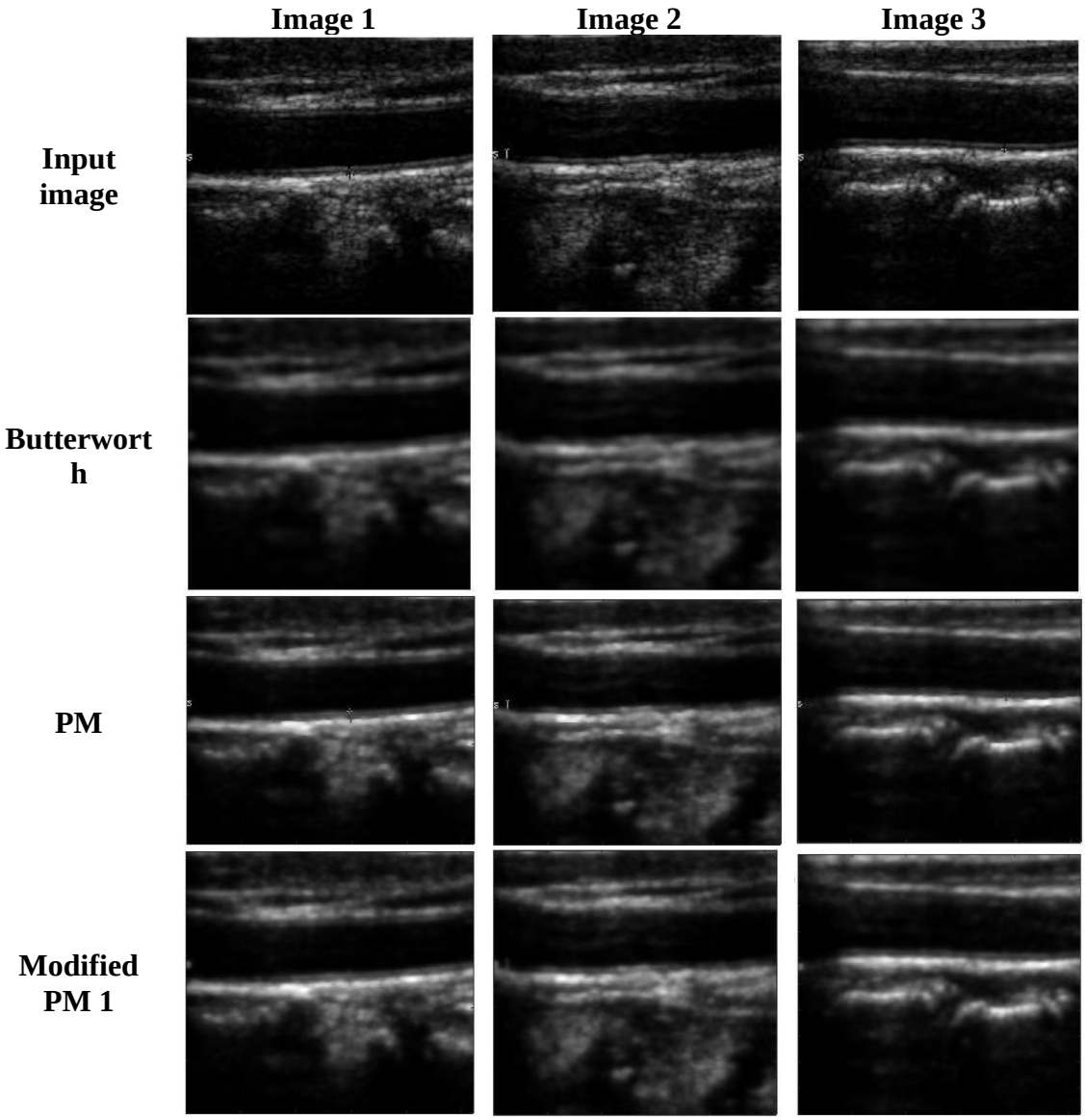

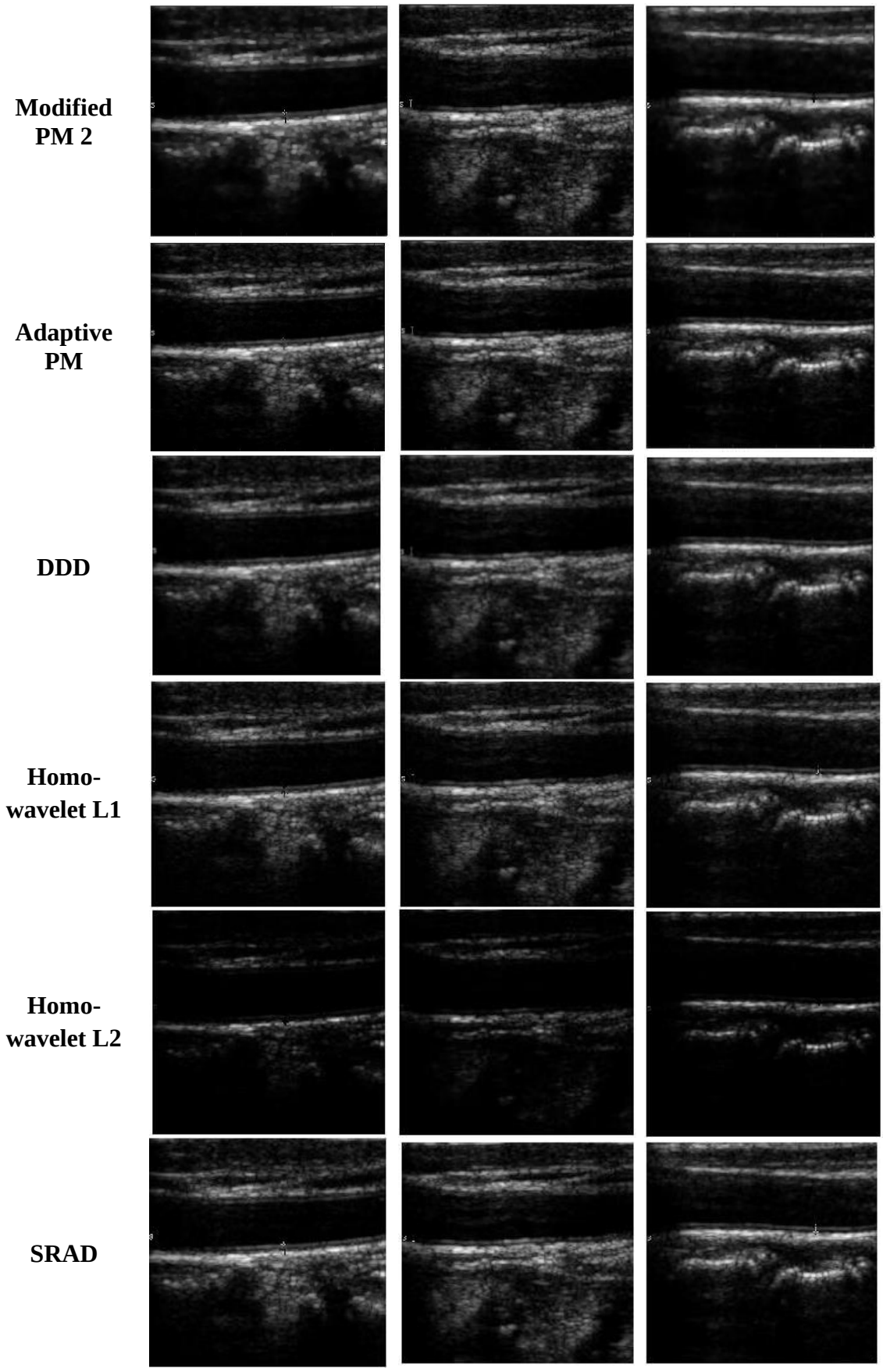
Modified PM 2
Adaptive PM
DDD
Homo-wavelet L1
Homo-wavelet L2
SRAD

TV

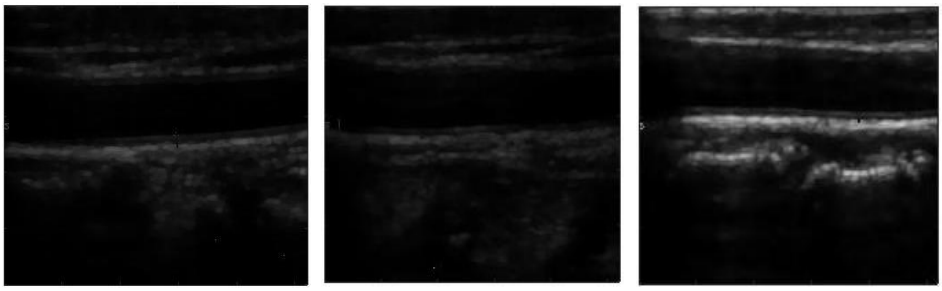

Figure 4 Output Images from Pre-processing

Figure 4 shows the pre-processed IVUS images using ten filters. A comparison is made between different despeckling methods in order to reduce speckle noise and make the images suitable for further analysis. Results from the experiments indicate that Homomorphic Wavelet Level 1, Modified PM 2, Adaptive PM, SRAD and DDD filtered images achieved higher SNR and PSNR values indicating successful despeckling. For Homomorphic Wavelet Level 1 and Adaptive PM, SSIM values are higher. When compared to other filters, the beta metric for SRAD and Modified PM 2 is higher, which indicates that edges are preserved well. Butterworth, Homomorphic Wavelet Level2 and DDD, on the other hand, did not preserve the edges, resulting in blurred images. Adaptive PM and SRAD maintained image perceptual quality, as shown by NIQE values.

The overall analysis shows that SRAD filter has achieved good SNR, PSNR values, indicating successful despeckling, as well as high Beta metric values for edge preservation.

6.2 Segmentation

By using performance metrics, such as JI, HD and DC, the automatic segmentation of IVUS images is compared to the ground truth images. Results from the segmentation algorithms are shown in Table 4.

a. Jaccard Index

Similarity between samples is assessed by calculating the Jaccard coefficient. In this analysis, the ground truth is compared with the segmentated output images. Mathematically JI is defined by Eqn.2. A_{GT} and $A_{seg\ img}$ are the vessel regions defined by ground truth and segmented region.

$$\left|\frac{A_{seg\ img} \cap A_{GT}}{A_{seg\ img} \cup A_{GT}}\right| = JI(A_{seg\ img}, A_{GT}) \qquad (2)$$

$A_{seg\ img}$ = Segmented Image

A_{GT} = Ground Image

b. Hausdorff Distance

The Hausdorff distance is a performance measure used to calculate the distance between two sets of points. In medical image segmentation, it is used for comparing ground truth images with segmentation output to allow them to be ranked together. The Hausdorff distance between two finite set points is given in Eqn. 3.

$$d_{HD}(X,Y) = \left(\frac{1}{X}\sum_{x\in X}\min d(x,y) + \frac{1}{Y}\sum_{y\in Y}\min d(x,y)\right)/2 \quad (3)$$

c. Dice Similarity Coefficient

Slice-by-slice comparison of segmented image to that of ground truth is evaluated using dice similarity coefficient. The overlapping areas of the segmented image are estimated using Eqn. 4 [27]. As these metrics accept the input image as binary, all the final segmented images and the ground truth are converted to binary form, and the evaluation is performed.

$$DC = 2\frac{|A_{seg\ img} \cap A_{GT}|}{|A_{seg\ img}| + |A_{GT}|} \quad (4)$$

Table 4.Comparison of performance using Jaccard Index (JI), Dice Coefficient (DC), and Hausdorff Distance (HD)

Algorithm	Test Image 1			Test Image 2		
	JI	DC	HD	JI	DC	HD
Watershed	0.9206	0.9014	5.2136	0.9105	0.9101	5.6201
Otsu's Thresholding [Hannah Sofian, 2015]	0.9012	0.8996	6.7895	0.9089	0.8989	6.0041
K Means K=1	0.8456	0.8012	5.7123	0.8956	0.8256	5.8941
K Means K=4	0.8899	0.8874	6.9874	0.8664	0.8881	6.9012
Fuzzy C Means	0.8574	0.8791	5.7894	0.8756	0.9008	4.5687
Global Region-based	0.9100	0.9014	4.9567	0.9075	0.9024	4.9568

segmentation						
Proposed Method (CNN)	**0.9562**	**0.9587**	**4.8080**	**0.9209**	**0.9156**	**4.4977**

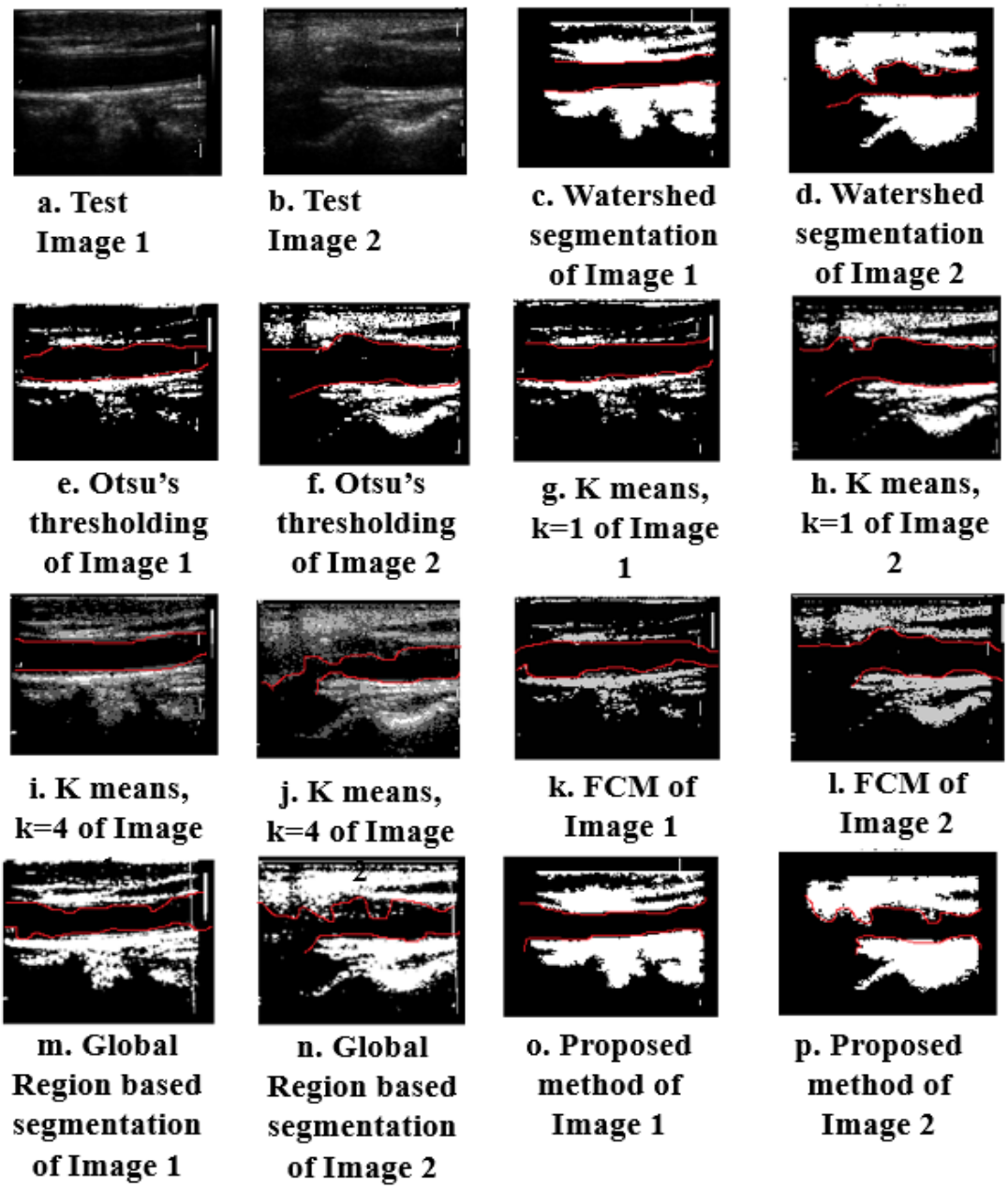
a. Test Image 1
b. Test Image 2
c. Watershed segmentation of Image 1
d. Watershed segmentation of Image 2
e. Otsu's thresholding of Image 1
f. Otsu's thresholding of Image 2
g. K means, k=1 of Image 1
h. K means, k=1 of Image 2
i. K means, k=4 of Image
j. K means, k=4 of Image
k. FCM of Image 1
l. FCM of Image 2
m. Global Region based segmentation of Image 1
n. Global Region based segmentation of Image 2
o. Proposed method of Image 1
p. Proposed method of Image 2

Figure 5 a and b are test images, c – p are the segmented images from implementing Watershed, Otsu's thresholding, K – Means (with k=1 and k=4), FCM, Global Region based and self-designed CNN architecture

The work compares the techniques used for segmenting the plaque region from an IVUS image. The precise segmentation can be used to measure the narrowing of the artery wall caused by plaque deposition. Considering the requirement of the

analysis, it is observed from the figure 5, the proposed CNN architecture gives a significant result compared to other techniques. It is noted that the values of JI and DC are 0.9562, 0.9587 respectively. The values are highly close to 1 compared to other segmenting algorithms. This indicates that the segmented regions are closer to the ground truth region.

6.3 Feature Extraction and Classification

Feature extraction must be non-redundant and carry information necessary for the classification process. The feature selection occurs after selection of the feature vectors. Feature vectors of a large number can lead to misclassification of images. Therefore, a more effective selection of features is necessary to improve classification accuracy. Textural features including mean, standard deviation, contrast, entropy, and energy are analyzed. The statistical measures used for analysis are shown in Table 5.

Table 5 Statistical Measures and its Mathematical Equation

Features	Equations
Mean	$\mu_i = \frac{1}{NM}\sum_{x=1}^{N}\sum_{y=1}^{M}\left\|D_j(x,y)\right\|$
Standard Deviation	$\sigma_i = \frac{1}{NM}\sum_{x=1}^{N}\sum_{y=1}^{M}\left\|D_j(x,y) - \mu_i\right\|^2$
Contrast	$\sum_{x=0}^{N-1}\sum_{y=0}^{N-1}\left\|x-y\right\|^2 p(x,y)$
Entropy	$\sum_{x=0}^{N-1}\sum_{y=0}^{N-1} p(x,y)\log\left(p(x,y)\right)$
Energy	$\sum_{x=0}^{N-1}\sum_{y=0}^{N-1} p(x,y)^2$

For the classification, 99 images from the IVUS dataset are used. The classifiers are trained on a dataset of 79 images using the extracted features vectors. The test dataset comprises of 20 images. Classifier performance is determined by calculating sensitivity, specificity, and accuracy.

- Sensitivity is the likelihood of the event that will be detected. The sensitivity equation is given below

$$Sensitivity = \frac{TP}{TP + FN} \quad (5)$$

- Specificity is the probability that the absence of the event getting identified. The equation of specificity is,

$$Specificity = \frac{TN}{TN + FP} \quad (6)$$

- Accuracy is the measure to check the functionality of a classifier.

$$Accuracy = \frac{TP + TN}{TP + FP + TN + FN} \quad (7)$$

Where *TP* is True Positive, *TN* is True Negative, *FP* is False Positive and *FN* is False Negative.

Table 6 shows the values of the performance metrics, calculated using the Eqn. (5) to (7), and Figure 6 shows the graphical representation of the performance of the classifiers. Among the four classifiers used, bagged trees showed higher accuracy of 96.2%, sensitivity of 92.6% and specificity of 96.8%.

Table 6 Performance Evaluation of Classifiers

Machine Learning Algorithm	Accuracy (%)	Sensitivity (%)	Specificity (%)
Support Vector Machine	91.1	83.33	95.39
K-Nearest Neighbour	96.2	91.26	96.37
Decision Tree	88.6	82.39	86.42
Bagged Trees	96.2	92.6	96.89

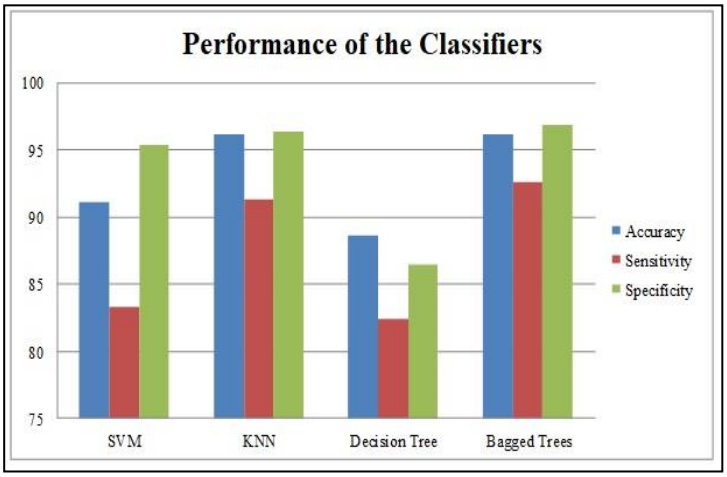

Figure 6 Performance Evaluation of the Classifier

6. CONCLUSION

This study is mainly focused on identifying plaque deposits in the Carotid Artery using IVUS images. Suitable speckle reducing filters are identified through applying ten filters to IVUS image dataset. SRAD filter gives a better despeckled image with good edge preservation. A machine learning-based segmentation method is used to identify the plaque deposited regions in arterial walls. Its performance is compared with other existing segmentation methods. A physician can determine the diagnostic procedure to be carried out further based on the segmented region. Finally, the plaque image is classified using techniques such as KNN, Support Vector Machine, Decision Tree and Bagged Tree.

7. ORGANIZATION OF RESEARCH

The thesis is organized as follows,

Chapter 1 describes about cardiovascular diseases, structure of carotid artery and discuss in detail about the Ultrasound imaging modality and its significance. **Chapter 2** studies and analyses the literature surveys which are related to this research work. **Chapter 3** describes about the pre-processing techniques implemented in reducing speckle noise in Intravascular Ultrasound Images**. Chapter 4** discuss the proposed segmentation method for plaque identification. Also, the other existing segmenting algorithms are discussed. **Chapter 5** presents various classifiers used for classification of IVUS dataset and the statistical measures used for performance analysis. **Chapter 6** discuss about the results obtained in detail. **Chapter 7** concludes the research work with the issues and future scope of the research.

REFERENCES

[1] Information on https://www.news-medical.net/news/20210127/COVID-19-will-impact-cardiovascular-disease-deaths-for-years-to-come-warn-experts.aspx.

[2] W. Insull Jr, "The Pathology of Atherosclerosis: Plaque Development and Plaque Responses to Medical Treatment," *Am. J. Med.* 122, S3–S14 (2009).

[3] Rajesh Mohan, R., Mridula, S., and MohananP, "Speckle Noise Reduction in Images using Wiener Filtering and Adaptive Wavelet Thresholding", *IEEE Region 10 Conference (TENCON)*(2016).

[4] Balocco, S., Gatta, C., Pujol, O., Mauri, J., and Radeva, P., "Speckle Reducing Bilateral Filtering", *Ultrasound in Medicine &Biology*. 36, 1353-63 (2010).

[5] Parminder, P.K., Tejinderpal, S, "Speckle Noise Reduction in Ultrasound Images: Performance Analysis and Comparison", *International Journal of Engineering Research & Technology*. Vol. 3 Issue 7 (2014).

[6] Lazrag, H., and Naceur, M. S, "Wavelet Filters Analysis for Speckle Reduction in Intravascular Ultrasound Images", *6th International Conference on Sciences of Electronics, Technologies of Information and Telecommunications (SETIT) (2012).*

[7] Yadav, A.K., Roy, R., Kumar, A.P., Kumar, C.S., and Dhakad S.K, "De-noising of Ultrasound Image using Discrete Wavelet Transform by Symlet Wavelet and Filters", *International Conference on Advances in Computing, Communications and Informatics (ICACCI)* (2015).

[8] Chinnathambi, V., Sankaralingam, E., Thangaraj, V., and Padma, S,"Despeckling of Ultrasound Images using Directionally Decimated Wavelet Packets with Adaptive Clustering", *IET Image Processing*. 13(1), 206–215 (2019).

[9] Vanithamani, R., and Umamaheswari, G. 2011, "Wavelet Based Despeckling of Medical Ultrasound Images with Bilateral Filter", *TENCON IEEE Region 10 Conference*, 389-393 (2011).

[10] Randhawa, S.K., Sunkaria, R.K. and Puthooran, E., "Despeckling of Ultrasound Images using Novel Adaptive Wavelet Thresholding Function", *Multidimensional System and Signal Processing*, 30, 1545–1561(2019).

[11] Dass, R., "Speckle Noise Reduction of Ultrasound Images Using BFO Cascaded with Wiener Filter and Discrete Wavelet Transform in Homomorphic Region", *Procedia Computer Science*. 132: 1543–1551(2018).

[12] Akl, A., and Yaacoub, C., "A Hybrid Filter for Image Despeckling with Wavelet-based Denoising and Spatial Filtering", *Third International Conference on Communications and Information Technology (ICCIT)*, 325-329 (2013).

[13] Olfa, M., and Nawres, K. 2014., "Ultrasound Image Denoising using a Combination of Bilateral Filtering and Stationary Wavelet Transform", *International Image Processing, Applications and Systems Conference*, 1-5 (0214).

[14] Loizou, C. P., Pattichis, C. S., Christodoulou, C. I., Istepanian, R. S. H., Pantziaris, M., and Nicolaides, A., "Comparative Evaluation of DespeckleFiltering in Ultrasound Imaging of the Carotid Artery", *IEEE Transactions on Ultrasonics, Ferroelectrics and Frequency Control,* 52(10): 1653–1669 (2005).

[15] Hengfei Cui, Yong Xia1, Yanning Zhang, "Supervised Machine Learning for Coronary Artery Lumen Segmentation in Intravascular Ultrasound Images", *International Journal for Numerical Methods in Biomedical Engineering,* 36 (2020).

[16] Paulo & Bulant, Carlos & Orlando, José & Maso Talou, Gonzalo & Alvarez, Alonso & Bezerra, Cristiano & Lemos, Pedro & Garcia-Garcia, Hector & Blanco, Pablo, "Automated Lumen Segmentation Using Multi-Frame Convolutional Neural Networks in Intravascular Ultrasound Datasets", *European Heart Journal - Digital Health,*(2020).

[17] Daniel Bos, Banafsheh Arshi, Quirijn J.A. van den Bouwhuijsen, M. Kamran Ikram, Mariana Selwaness, Meike W. Vernooij, Maryam Kavousi, Aad van der Lugt, "Atherosclerotic Carotid Plaque Composition and Incident Stroke and Coronary Events", *Journal of The American College of Cardiology,* Vol. 77, No. 11 (2021).

[18] Park, Jung-Eun&Kweon, Jihoon& Kang, Do-Yoon & Lee, Pil&Ahn, Jung-Min & Kang, Soo-Jin& Park, Duk-Woo & Lee, Sung Won & Lee, Cheol & Kim, Jae Seung & Kim Y.H., "Deep Learning Segmentation of Lumen and Vessel on IVUS Images", *Journal of the American College of Cardiology*, (2021).

[19] Z. Zhou, H. Wang, W. Shang and L. Zhang, "Image Segmentation Algorithms Based on Convolutional Neural Networks," *17th International Conference on Computer and Information Science (ICIS),* (2018).

[20] Fabrizio Sottile, Silvia Marino, PlacidoBramanti and LillaBonanno, "Validating a Computer-Aided Diagnosis System for Identifying Carotid Atherosclerosis",*International Congress on Image and Signal Processing* (2013).

[21] Zhou, Z., Guo, Z., Dong, G., Sun, J., Zhang, D., and Wu, B. 2015. A Doubly Degenerate Diffusion Model Based on the Gray Level Indicator for Multiplicative Noise Removal. *IEEE Transactions on Image Processing*, 24(1): 249–260 (2015).

[22] Gungor, A., and Karagoz, I., "Comparing Non-homomorphic and Homomorphic Wavelet Filtering Techniques for Speckled Images", *International Journal of Computer Theory and Engineering,* 8(5),393-397 (2016).

[23] Yu, Y., and Acton, S.T., "Speckle Reducing Anisotropic Diffusion", *IEEE Transaction on Image Processing*, 11, 1260-1270 (2002).

[24] Choi, H., and Jeong, J., "Speckle Noise Reduction in Ultrasound Images using SRAD and Guided Filter", *International Workshop on Advanced Image Technology (IWAIT) (2018).*

[25] Anthony Bua, "Edge-aware Nonlinear Diffusion-driven Regularization Model",MATLAB Central File Exchange. https://www.mathworks.com/matlabcentral/fileexchange/74536-edge-aware-nonlinear-diffusion-driven-regularization-model (2021).

[26] Aydin, O.U., Taha, A.A., Hilbert, A., "On the Usage of Average Hausdorff Distance for Segmentation Performance Assessment: Hidden Error when Used for Ranking", *European Radiology Experimental*, (2021).

[27] Xin Yang, JiaoyingJin, MenglingXu, Huihui Wu, Wanji He, Ming Yuchi, and Mingyue Ding, "Ultrasound Common Carotid Artery Segmentation Based on Active Shape Model", *Computational and Mathematical Methods in Medicine*,(2013).

PUBLICATION DETAILS

Journal Publications:

Sl.No.	Title of the Paper	Journal	Volume/Page. No./Month and Year of Publication
1.	A Comparison on Speckle Noise Suppression Algorithm For Intravascular Ultrasound (IVUS) Images	Indian Journal of Computer Science and Engineering **(SCOPUS INDEXED)**	Volume 12, No. 3, May-Jun 2021, Page No. 634 – 640 DOI : 10.21817/indjcse/2021/v12i3/211203130
2.	Segmentation of Carotid Artery from Intravascular Ultrasound (IVUS) Images Using Deep Learning Techniques for Plaque Identification	ICTACT Journal on Image and Video Processing **(UGC CARE I)**	Volume 12, Issue 3, February 2022, pp. 2638 – 2643 DOI: 10.21917/ijivp.2022.0374
3.	Detection of Plaques in Artery Wall Using Intravascular Ultrasound Images for Diagnosis of Coronary Artery Diseases	Journal of Theoretical and Applied Information Technology **(SCOPUS INDEXED)**	Volume 100, No.4, pp. 914 – 926 February 2022
4.	Segmentation of Intima Media Thickness in Intravascular Ultrasound (IVUS) Images or Detection of Atherosclerosis	Biomedical and Pharmacology Journal, (**SCOPUS INDEXED)**	Volume 15, No.3, pp. 1539 – 1549, September 2022. https://dx.doi.org/10.13005/bpj/2492

Conference Presentation:

S. No.	Title of the Paper	Name of the Conference and Venue	Date
1.	Diagnosis of Coronary Artery Diseases and Carotid Atherosclerosis using Intravascular Ultrasound Images	International Conference on Artificial Intelligence **SLAAI – 2018**, conducted by University of Moratuwa, Sri Lanka.	20.12.2018
2.	A Review on Pre-processing and Segmentation Techniques in Carotid Artery Ultrasound Images	International Conference on Evolutionary Computing and Mobile Sustainable Networks (ICECMSN -2021) organised by Department of CSE and ECE, RV Institute of Technology and Management, Bengaluru.	28.09.2021 -29.09.2021

Book Chapters:

S. No.	Title of the Book Chapter	Book Title	Volume/Issue/ Page No./ Year
1.	Diagnosis of Coronary Artery Diseases and Carotid Atherosclerosis Using Intravascular Ultrasound Images	Communications in Computer and Information Science ISBN:978-981-13-9129-3	Series No. 890, pp. 281–288, 2019 https://doi.org/10.1007/978-981-13-9129-3_20
2.	A Review on Preprocessing and Segmentation Techniques in Carotid Artery Ultrasound Images	Lecture Notes on Data Engineering and Communications Technologies, book series (LNDECT) in the book titled Evolutionary Computing and Mobile Sustainable Networks	Volume 116, pp. 883 - 897, March 2022